Journal of Alloys and Compounds 503 (2010) 286–290

Contents lists available at ScienceDirect

Journal of Alloys and Compounds

journal homepage: www.elsevier.com/locate/jallcom

Effects of trace C addition on the microstructure and refining efficiency of Al–Ti–B master alloy

P.T. Li, X.G. Ma, Y.G. Li, J.F. Nie, X.F. Liu*

Key Laboratory for Liquid–Solid Structural Evolution and Processing of Materials, Ministry of Education, Shandong University, Jinan 250061, PR China

ARTICLE INFO

Article history:
Received 10 March 2010
Received in revised form 26 April 2010
Accepted 29 April 2010
Available online 11 May 2010

Keywords:
Al–Ti–B master alloy
Grain refinement
TiC
TiB_2

ABSTRACT

The effects of a trace amount of C addition on the microstructure and refining performance of Al–Ti–B master alloy were studied and the Al–5Ti–0.8B–0.2C master alloy was prepared. Particles were extracted from the Al–5Ti–1B and Al–5Ti–0.8B–0.2C master alloys. In the Al–5Ti–1B master alloy, TiB_2 particles exhibit hexagonal platelet and layered stacking morphologies, and agglomerate seriously in grain boundaries. After a trace amount of C is added, many paragenetic particles form in the Al–5Ti–0.8B–0.2C master alloy. They are composed of TiB_2 particles and small TiC particles. The small TiC particles grow on the surface of TiB_2 particles or are enchased in TiB_2 particles. The existence of TiC particles weakens the TiB_2 particle agglomerations obviously. Due to the microstructure improvement, the Al–5Ti–0.8B–0.2C master alloy shows much better refining performance than the Al–Ti–B master alloy. The average grain size of α-Al refined by 0.2 wt.% the prepared Al–5Ti–0.8B–0.2C master alloy is about 190 μm. In addition, the refining efficiency of the Al–5Ti–0.8B–0.2C does not fade within 60 min.

1. Introduction

Grain refinement is considered to be an important melt treatment during casting of aluminium alloys [1] and the introduction of inoculating particles into melts is the most widely used way to achieve small uniformly distributed equiaxed grains, leading to high toughness, high yield strength, excellent formability and improved machinability [2]. Al–Ti–B ternary master alloys, in particular Al–5%Ti–1%B (all compositions quoted in this work are in wt.% unless otherwise stated), have been widely used as aluminium grain refiners over the past several decades [3,4], and the most popular method for preparing Al–Ti–B master alloys is feeding a mixture of KBF_4 and K_2TiF_6 salts to molten aluminium between 750 and 850 °C [2–4]. However, Al–Ti–B master alloys and the "halide salt" route still have several problems, such as agglomeration of the borides and low content of B and Ti in the fluoride [2,5]. Finally, perhaps the greatest challenge facing grain refinement is the very low efficiency, with at best 1% of the added TiB_2 particles acting as nucleation substrates for grain nucleation [6,7].

Extensive studies have been conducted in recent decades by changing the raw materials and preparation methods. For example, Yücel B prepared a more effective Al–5Ti–1B by replacing of KBF_4 with $Na_2B_4O_7$ or B_2O_3 via SHS (self-propagating high-temperature synthesis) technology [8,9]; Zhang fabricated a new kind of Al–5Ti–1B by rapid cooling giving better refining efficiency [10]. However, these alloys still cannot replace the traditional Al–Ti–B master alloys because such challenges as the need for complex processing equipment and sensitivity to contamination of products remain to be solved.

Interestingly, Nie [11] prepared a high-performance Al–5Ti–0.3C–0.2B master alloy based on Al–Ti–C system, using a melt reaction method and observed an improvement in the refining efficiency due to the more stable TiC particles doped with B. In this paper, a trace amount of C was added to an Al–Ti–B alloy resulting in the formation of an Al–5Ti–0.8B–0.2C master alloy. The effect on the grain refining efficiency of the C containing master alloy when added to commercially pure aluminium was compared to the conventional Al–5Ti–1B master alloy. The Al–Ti–B–C master alloy showed a considerably higher grain refining efficiency and stability and may be relevant for industrial applications where long holding times and fading of the refining effect are encountered.

2. Experimental procedure

In order to study the effects of a trace amount of C addition on the microstructure and refining efficiency of master alloy, Al–5Ti–1B (hereinafter referred to as Al–Ti–B) master alloy and Al–5Ti–0.8B–0.2C (hereinafter referred to as Al–Ti–B–C) master alloy were fabricated in this study. The mass fraction of B in the Al–Ti–B master alloy and the mass fraction of B and C in the Al–Ti–B–C master alloy were designed to be equal. The Al–Ti–B master alloy was prepared using pure Ti (99.5%), Al–3B master alloy and commercial pure aluminium (99.7%). The Al–Ti–B–C master alloy was prepared using pure Ti, graphite powder (99.85%, 10 μm), Al–3B master alloy and commercial pure aluminium. Both of the Al–Ti–B and Al–Ti–B–C master alloys were prepared using a melt reaction method in a medium frequency furnace.

* Corresponding author. Fax: +86 531 88395414.
E-mail address: xfliu@sdu.edu.cn (X.F. Liu).

0925-8388/$ – see front matter © 2010 Elsevier B.V. All rights reserved.
doi:10.1016/j.jallcom.2010.04.251

Grain refining tests were carried out by adding 0.2% Al–Ti–B or 0.2% Al–Ti–B–C master alloy into commercial pure aluminium melts at 730 °C. The melts were then poured into a pre-heated KBI cylindrical steel mold (50 mm in diameter and 25 mm in height) to gain samples at 5 min, 15 min, 30 min, 45 min and 60 min, respectively. Then, the bottom surfaces of the refined samples were etched by a reagent (60% HCl + 30% HNO_3 + 5% HF + 5% H_2O, the compositions here are in volume fraction). At last, the macrostructure photos were taken from each sample by a high scope video microscope (HSVM, KH-2200), and the average grain sizes were calculated by the linear intercept method.

In order to observe the three-dimensional morphologies of particles in the Al–Ti–B and Al–Ti–B–C master alloys, the particles were extracted by a special extraction method [12] with some modification. Firstly, the aluminium matrix was dissolved in a solution of 10% HCl. Next, the particles in the solution were centrifuged by a centrifugal extractor, and then the collected sediments were rinsed with distilled water and ethanol for several times. The metallographic specimens and extracted powders were analyzed by X-ray diffraction (XRD, Rigaku D/max-rB) and field emission scanning electron microscope (FESEM, SU-70).

3. Results and discussion

3.1. Microstructures and microanalysis of the master alloys

The Al–Ti–B–C master alloy mainly contains four kinds of phases: α-Al, $TiAl_3$, TiB_2 and TiC, as shown in the XRD result of Fig. 1.

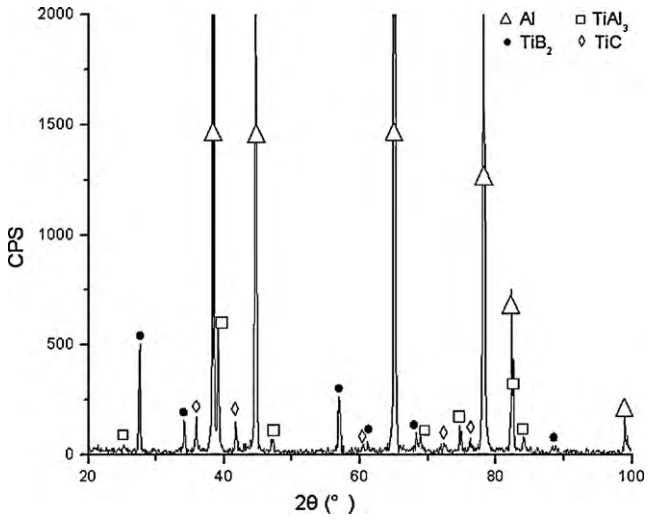

Fig. 1. X-ray diffraction patterns of the Al–Ti–B–C master alloy.

Fig. 2 shows the microstructures of the Al–Ti–B and Al–Ti–B–C master alloys. Both of them are mainly composed of plate-like $TiAl_3$ and numerous particles distributing in α-Al grain boundaries. In order to further identify the phases and their specific distributions, local areas of the grain boundaries were magnified (Fig. 2(c) and (d)), and FESEM line-scanning analysis was carried out along the line A–B in Fig. 3. The big particles with the size over 1 μm are TiB_2 and the submicron particles are TiC, as can be seen from the diffraction peaks in Fig. 3(b). It can be also found that TiB_2 particles in the Al–Ti–B master alloy (Fig. 2(c)) agglomerated seriously, while the particle agglomerations in the Al–Ti–B–C master alloy were weakened obviously, and particles became unattached with each other. Previous work revealed that TiC particles in Al–Ti–C master alloy are more dispersive than TiB_2 particles in Al–Ti–B system [13–15]. When Ti is added into the melt during preparing the Al–Ti–B–C master alloy, TiC and TiB_2 particles form rapidly. They are alternately distributed in the Al–Ti–B–C master alloy, so the TiC particles will act as obstacles to hinder the form of TiB_2 agglomerations, leading to the relatively distributed particles. Furthermore, the amount of second phase particles in the Al–Ti–B–C master alloy (Fig. 2(b)) are obviously larger than that in the Al–Ti–B master alloy (Fig. 2(a)), although the total mass fraction of B and C in the Al–Ti–B–C is equal to that of B in the Al–Ti–B. In order to prove this point, quantitative analysis was conducted. 10.019 g Al–Ti–B and 10.031 g Al–Ti–B–C master alloys were eroded and the second phase particles were

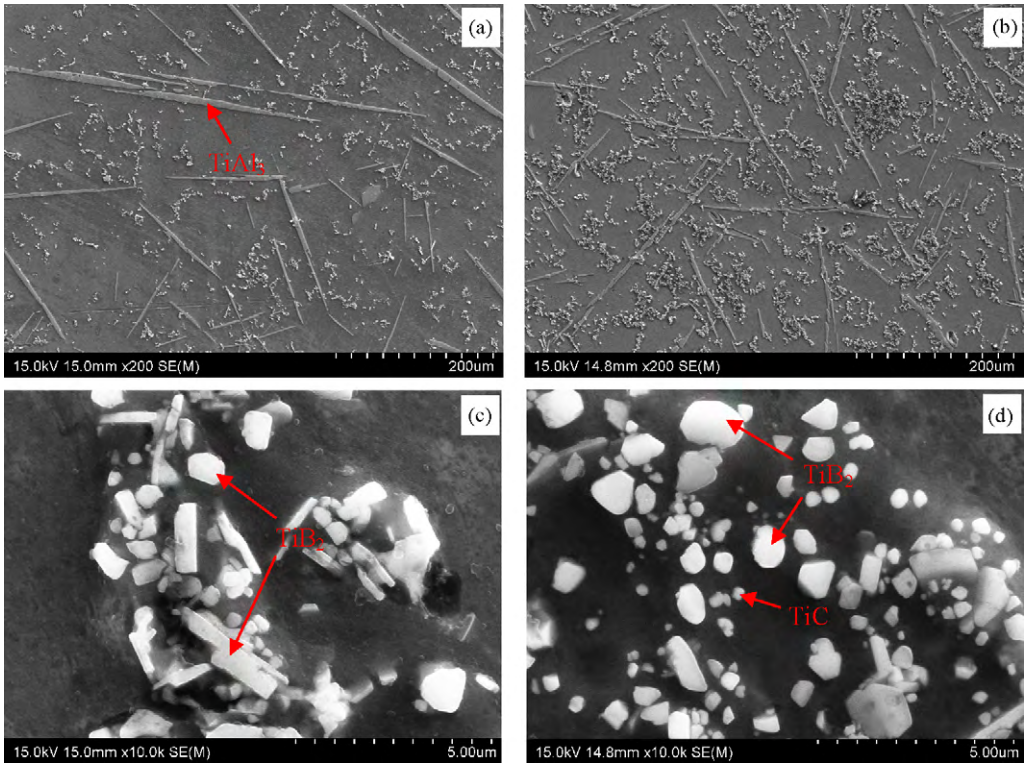

Fig. 2. Microstructures of Al–Ti–B and Al–Ti–B–C master alloys: (a) low magnification of the Al–Ti–B master alloy; (b) low magnification of the Al–Ti–B–C master alloy; (c) high magnification of the Al–Ti–B master alloy; (d) high magnification of the Al–Ti–B–C master alloy.

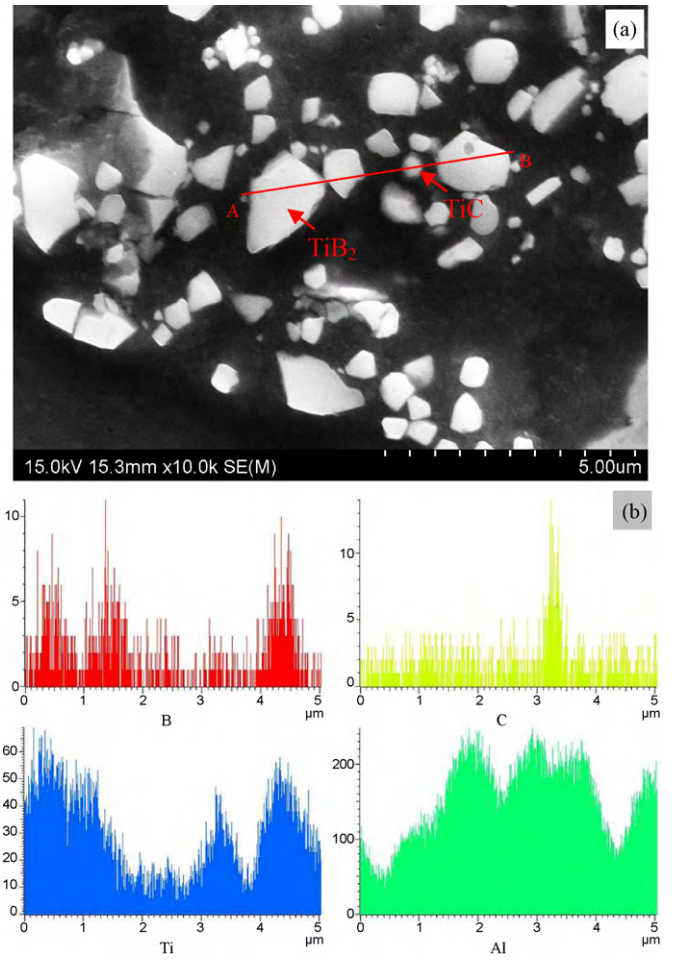

Fig. 3. Line-scanning analysis of particles in the Al–Ti–B–C master alloy: (a) SEI image; (b) line-scanning analysis along A–B.

collected. The weights of the extracted particles in the Al–Ti–B and Al–Ti–B–C are 0.871 g and 0.884 g respectively. Moreover, since the size of TiC is much smaller than that of TiB_2, it can be concluded that the number of second phase particles in the Al–Ti–B–C master alloy is actually larger than those in the Al–Ti–B master alloy.

In order to observe the morphology of particles in the Al–Ti–B and Al–Ti–B–C master alloys, TiC and TiB_2 were extracted by eroding the Al matrix away. Fig. 4 shows the typical morphologies of particles extracted from the two master alloys. TiB_2 particles in the Al–Ti–B master alloy mainly exhibit two kinds of morphologies: hexagonal platelet (Fig. 4(a)) and layered stacking (Fig. 4(b)). The crystal structure of TiB_2 is hexagonal close-packed, and the {0 0 0 1} planes share the highest surface atomic density, the lowest surface energy and the slowest growth rate. Therefore the growth of {0 0 0 1} planes will be limited and the face will appear at last. Consequently, TiB_2 particles would exhibit hexagonal platelet morphologies under normal conditions as shown in Fig. 4(a), and the large surface of TiB_2 particles is the {0 0 0 1} close-packed plane. However, the TiB_2 particle in Fig. 4(b) is composed of multiple thin platelets with the thickness less than 0.1 μm. There are displacements between neighboring thin platelets, which is beneficial to the formation of a ladder structure along a certain direction. It is believed that the formation of the layered stacking morphology is related to the high atomic diffusion rate and reaction rate caused by the high reaction temperature [16]. Apart from the above two kinds of morphologies, a large amount of particles exhibit irregular morphologies (Fig. 4(c)) in the Al–Ti–B–C master alloy. Actually they are paragenetic particles including TiB_2 and TiC particles (identified by point analysis). Small TiC particles grow on the TiB_2 particle surfaces or are enchased in TiB_2 particles and form many paragenetic particles. Ogwu and Davies mentioned in their article [17] that there allows coherence structure between the most densely packed lattice planes of TiC and TiB_2 particles. The formation of paragenetic particles is due to this character of TiC and TiB_2 particles. When Ti was added into the melt, the dissolved Ti reacted with B from the Al–3B master alloy to form TiB_2, while C and Ti reacted to form TiC. These two reactions mainly occurred in the Ti-rich regions simulta-

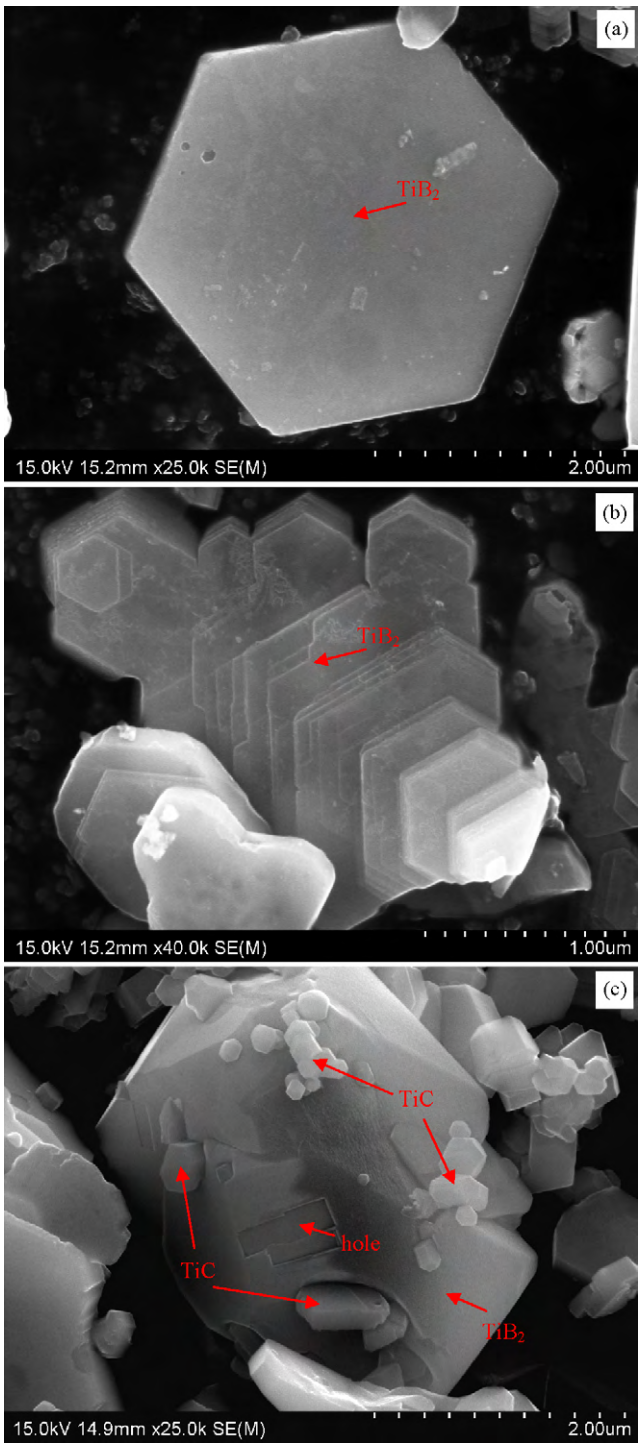

Fig. 4. SEM micrographs of extracted particles from Al–Ti–B and Al–Ti–B–C master alloys: (a and b) TiB_2 particles from the Al–Ti–B master alloy; (c) particle clusters from the Al–Ti–B–C master alloy.

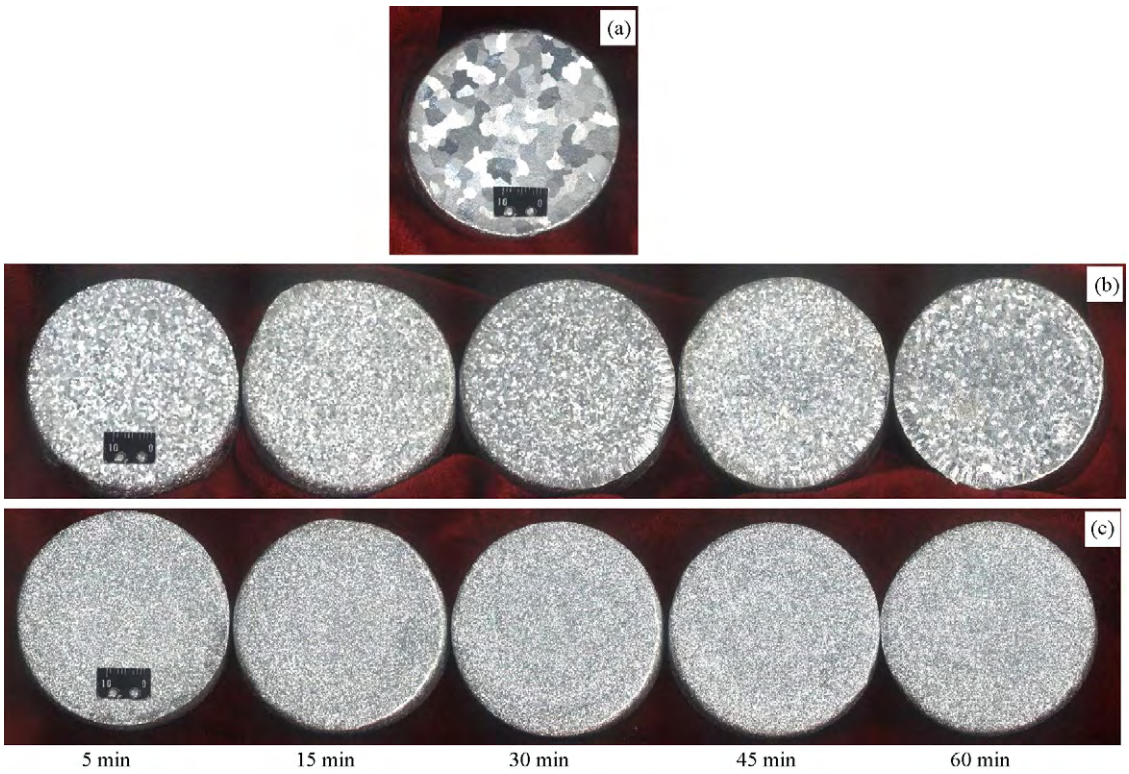

Fig. 5. The grain performance of the Al–Ti–B or Al–Ti–B–C master alloy: (a) without grain refiner; (b) addition of 0.2% Al–Ti–B master alloy holding for 5 min, 15 min, 30 min, 45 min and 60 min; (c) addition of 0.2% Al–Ti–B–C master alloy holding for 5 min, 15 min, 30 min, 45 min and 60 min.

neous. The TiB_2 particles are much bigger than the TiC particles in the Al–Ti–B–C master alloy, as shown in Figs. 3 and 4. TiC particles may be packed by TiB_2 particles or grow on the surface of TiB_2 particles when the particles grow up, as shown in Fig. 4(c), because of the coherence structure between TiC and TiB_2 particles. The interfaces of TiC and TiB_2 particles have high interfacial energies and are easy to be eroded, leading to TiC particles falling off from TiB_2 particles and the formation of holes (Fig. 4(c)).

3.2. Grain refinement of master alloys

Fig. 5 shows the macrostructures of 99.7% commercial pure aluminium refined by the Al–Ti–B or Al–Ti–B–C master alloy after 5 min, 15 min, 30 min, 45 min and 60 min holding at 730 °C, respectively. The grain size of commercial purity aluminium without adding grain refiners is coarse, as shown in Fig. 5(a). The coarse grains of aluminium are obviously refined to small equiaxed grains by adding either the Al–Ti–B or Al–Ti–B–C master alloy. Notably, the average grain size of α-Al refined by the Al–Ti–B–C master alloy is about 190 μm which is much finer than those refined by the Al–Ti–B master alloy. The present results indicate that the grain refining performance of the Al–Ti–B master alloy has been significantly improved by adding a trace amount of C during the preparing process. Fig. 6 displays the average grain size variation as a function of holding time. For the pure aluminium refined by the Al–Ti–B–C master alloy, the average grain size is below 200 μm within 60 min holding, while that of aluminium refined by the Al–Ti–B master alloy is larger than 300 μm and coarsening rapidly with time.

The refining efficiency and stability of the grain refiners are not only related to the number of second phase particles acting as potential nucleation substrate of α-Al, but also concerned with their morphologies and distributions [13–15,18–20]. According to the classical nucleation theory, the smooth particle surfaces are difficult for Ti concentrating, while morphology with nooks is good for Ti enriching [21]. The nooks in particles with high Ti contents are the most effective nucleation substrates for α-Al. So the irregular morphologies of particles are helpful to improve the nucleation efficiency [22]. Furthermore, the distributions of the second phase particles in master alloys also have great influence on the refining efficiency. If the second phase particles agglomerated, it is hard for them to distribute after the master alloy being added to Al melts. The agglomerations are likely to deposit to the bottom, causing the number of potential nuclei to decrease, and the refining efficiency fade eventually [5,23].

In this study, the number of the second phase particles increased significantly after adding a trace amount of C. The increase of particles means more potential nuclei produced and refining efficiency improved. Meanwhile, the particle agglomerations were weakened

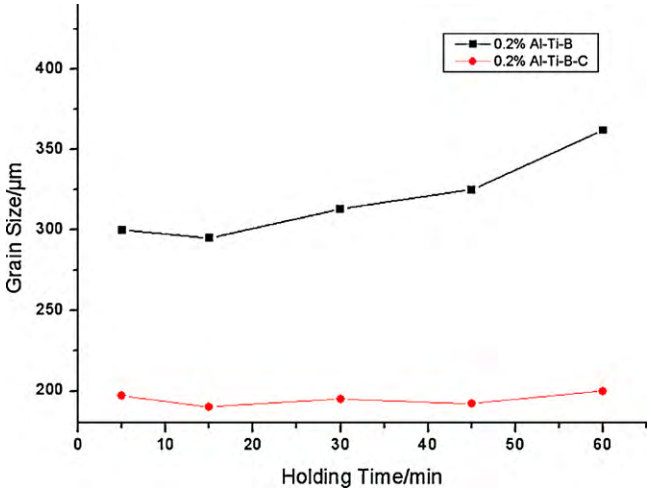

Fig. 6. Grain refining efficiencies of Al–Ti–B and Al–Ti–B–C master alloys at 730 °C.

obviously and particles became unattached in the Al–Ti–B–C master alloy. This better distribution assures enough particles to serve as nuclei for α-Al and makes particles difficult to gather and deposit during the refining process. Besides, many irregular paragenetic particles formed in the Al–Ti–B–C master alloy. The nooks of the paragenetic particles are in favor of Ti enrichment and make it easier for α-Al to grow on the surfaces of particles during the nucleation process. The trace amount of C addition into Al–Ti–B master alloy made great improvement in the refining efficiency and antifade ability of master alloy. It is attributed to the increased particle number, improved particle distributions and good particle morphologies.

4. Conclusion

(1) Al–5Ti–0.8B–0.2C master alloy was obtained by adding a trace amount of C during the preparation of Al–Ti–B master alloy. In Al–5Ti–0.8B–0.2C the particle agglomerations were weakened obviously, and particles became unattached with each other.
(2) The TiB_2 particle morphologies in Al–5Ti–1B master alloy are mainly hexagonal platelet and layered stacking. Apart from these kinds of TiB_2, in Al–5Ti–0.8B–0.2C master alloy, another kind of TiB_2 particles with irregular morphologies formed. Small TiC particles grow on the surfaces of TiB_2 particles or are enchased in TiB_2 particles and form many paragenetic particles.
(3) Al–5Ti–0.8B–0.2C master alloy possesses much better grain refining performance than Al–5Ti–1B master alloy. The average grain size of commercial pure aluminum refined by 0.2 wt.% Al–5Ti–0.8B–0.2C master alloy was about 190 μm, which is much smaller than the grain with the size of 300 μm refined by Al–Ti–B master alloy. Moreover, the refinement efficiency of Al–5Ti–0.8B–0.2C will not fade holding 60 min in the molten aluminum.

Acknowledgments

This work was supported by a grant from National Science Fund for Distinguished Young Scholars (no. 50625101), Key Project of Science and Technology Research of Ministry of Education of China (no. 106103) and "Taishan Scholar" Construction Project for financial support of Shandong Province in China.

References

[1] P.S. Mohanty, J.E. Gruzleski, Acta Metal. Mater. 43 (1995) 2001–2012.
[2] B. Yücel, J. Alloys Compd. 440 (2007) 108–112.
[3] T.S. Krishnana, P.K. Rajagopalana, B.R. Gundb, J. Krishnanb, D.K. Bosec, J. Alloys Compd. 269 (1998) 138–140.
[4] M.A. Easton, D.H. Stjohn, Acta Mater. 49 (2001) 1867–1878.
[5] P.L. Schaffer, A.K. Dahle, Mater. Sci. Eng. A 413–414 (2005) 373–378.
[6] A.L. Greer, A.M. Bunn, A. Tronche, P.V. Evans, D.J. Bristow, Acta Mater. 48 (2000) 2823–2835.
[7] Z.Q. Wang, X.F. Liu, Y.H. Liu, et al., Mater. Sci. Technol. 19 (2003) 1709–1714.
[8] B. Yücel, J. Alloys Compd. 443 (2007) 94–98.
[9] B. Yücel, J. Alloys Compd. 458 (2008) 271–276.
[10] Z.H. Zhang, X.F. Bian, Y. Wang, X.F. Liu, Mater. Sci. Eng. A 352 (2003) 8–15.
[11] J.F. Nie, X.F. Liu, X.G. Ma, J. Alloys Compd. 491 (2010) 113–117.
[12] C.P. Liu, F.S. Pan, W.Q. Wang, Mater. Sci. Forum 546–549 (2007) 395–398.
[13] H.M. Ding, X.F. Liu, L.N. Yu, G.Q. Zhao, Scripta Mater. 57 (2007) 575–578.
[14] M. Vandyoussefi, J. Worth, A.L. Greer, Mater. Sci. Technol. 16 (2000) 1121–1128.
[15] A.R. Kennedy, D.P. Weston, M.I. Jones, C. Enel, Scripta Mater. 42 (2000) 1187–1192.
[16] S.B. Jin, P. Shen, B.L. Zou, Q.C. Jiang, Cryst. Growth Des. 9 (2009) 646–649.
[17] A.A. Ogwu, T.J. Davies, Phys. Stat. Sol. A. 153 (1996) 101–116.
[18] X.F. Liu, Z.Q. Wang, Z.G. Zhang, X.F. Bian, Mater. Sci. Eng. A 332 (2002) 70–74.
[19] X.G. Ma, X.F. Liu, H.M. Ding, J. Alloys Compd. 471 (2009) 56–59.
[20] B.S. Murti, S.A. Kori, K. Venkateswarlu, R.R. Bhat, M. Chakraborti, J. Mater. Process. Technol. 89–90 (1999) 152–158.
[21] J.G. Li, M. Huang, M. Ma, W. Ye, D.Y. Liu, et al., Trans. Nonferrous Met. Soc. China 16 (2006) 242–253.
[22] W.H. Jiang, X.L. Han, Spec. Cast. Nonferrous Alloy 01 (1997) 19–22.
[23] Y.F. Han, K. Li, J. Wang, D. Shu, B.D. Sun, Mater. Sci. Eng. A 405 (2005) 306–312.